ORGANOMETALLICS

Article

Cite This: *Organometallics* 2019, 38, 3338−3348

pubs.acs.org/Organometallics

E-Selective Synthesis and Coordination Chemistry of Pyridine-Phosphaalkenes: Five Ligands Produce Four Distinct Types of Ru(II) Complexes

Mika L. Nakashige,[†] Jarin I. P. Loristo,[†,∥] Lesley S. Wong,[†,∥] Joshua R. Gurr,[†] Timothy J. O'Donnell,[†] Wesley Y. Yoshida,[†] Arnold L. Rheingold,[§] Russell P. Hughes,[‡] and Matthew F. Cain*[,†]

[†]Department of Chemistry, University of Hawai'i at Mānoa, 2545 McCarthy Mall, Honolulu, Hawaii 96822, United States

[‡]6128 Burke Laboratory, Department of Chemistry, Dartmouth College, Hanover, New Hampshire 03755, United States

[§]Department of Chemistry, University of California, San Diego, 9500 Gilman Drive, La Jolla, California 92093, United States

Supporting Information

ABSTRACT: Pyridine-phosphaalkene (PN) ligands **2a−e** were prepared in an *E*-selective fashion using phospha-Wittig methodology. Treatment of these five ligands, varying only in their 6-substituent with $RuCl_2(PPh_3)_3$, produced four distinct types of coordination complexes: pyridine-phosphaalkene-derived **3b,d**, cyclized **4e**, and six-coordinate **5a** and **6c**. Prolonged heating of **3b,d** in THF resulted in C−H activation of the Mes* group and cyclization to give **4b,d** featuring a bidentate pyridine-phospholane ligand bound to the metal center. Complex **5a**, also possessing a newly formed phospholane ring, contained a different spatial arrangement of donors to Ru(II) with an agostic Ru−H−C interaction serving as the sixth donor to the transition metal center. Ligands **2b,d,e** and Ru(II) complexes **3b, 4b,e** and **5a** were all characterized by X-ray crystallography. Six-coordinate **6c** featured a structure similar to **4b,d,e**, but with the CF_3 substituent acting as a weakly bound sixth ligand to the Ru(II) center, as observed by $^{31}P\{^1H\}$ and ^{19}F NMR spectroscopy. The calculated structure of **6c** established that the closest Ru- - -F contact was at 2.978 Å.

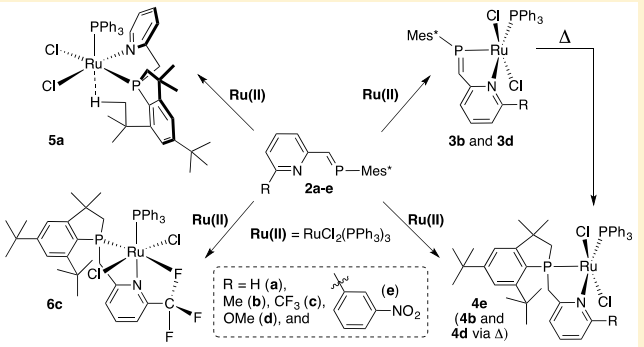

INTRODUCTION

Phosphaalkene-based ligands featuring low-lying π^* orbitals and large P substituents have emerged as a successful class of pincers for stabilizing low-coordinate and electron-rich metal centers,[1] some in unusual geometries including trigonal-monopyramidal **A**[2] and T-shaped **B** (Scheme 1, top).[3]

The versatility of the P═C unit is remarkable, functioning as a strong π acceptor,[4] as an electron reservoir,[5] and as a site for both external nucleophilic attack[6] and intramolecular C−H activation and cyclization.[7] These cyclizations generally afford phospholanes,[8] and in the case of phosphaalkene-derived PCP pincer **C**,[9] a catalytic amount of $[Pt(PCy_3)_2]$ promotes the formation of bis(phospholane) **D**.[7] Interestingly, the PNP analogue **E**[10] was far more resistant to double cyclization, requiring forcing conditions (80 °C, 11 days) to produce **F** (Scheme 1, bottom).[11] However, a single cyclization of bis(phosphaalkene) **E** occurs readily at metal centers,[12] affording square-planar **G**[12] and octahedral **H**[11] with a modified PNP pincer featuring phospholane, pyridine, and phosphaalkene donors. Akin to the metal complexes reported by Milstein that are supported by neutral, tridentate pincers bearing a central N-heterocyclic donor,[13] treatment of **G** and **H** with base results in deprotonation of the benyzlic arm and subsequent dearomatization of the pyridine functionality and isolation of **I** and **J** (Scheme 2).[11,12]

Scheme 1. Unusual Metal Geometries Supported by Phosphaalkene-Based PNP Pincers (Top) and Intramolecular C−H Activation and Cyclization of Phosphaalkenes Catalyzed by $[Pt(PCy_3)_2]$ (Bottom)

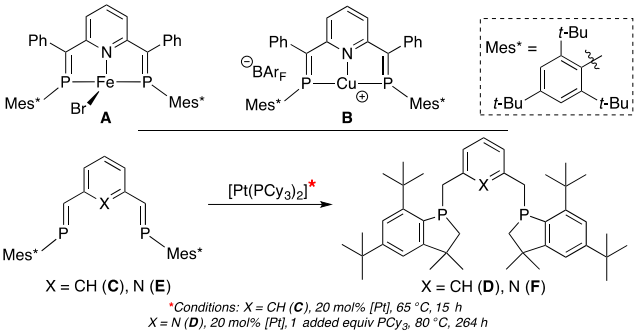

Received: June 25, 2019
Published: August 22, 2019

DOI: 10.1021/acs.organomet.9b00425
Organometallics 2019, 38, 3338−3348

Scheme 2. Synthesis of Dearomatized Pincer Complexes I and J

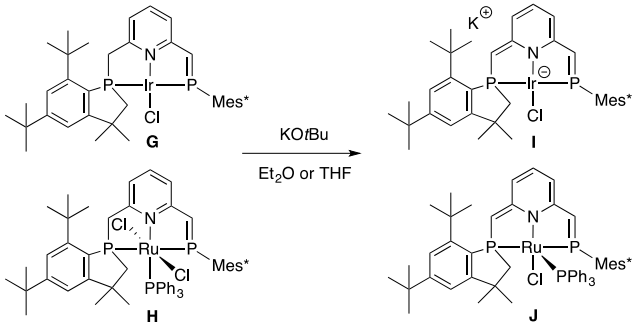

Dearomatized **I** is capable of facilitating the N−H activation of ammonia and other primary amines,[12,14] while a related analogue of **J** promotes catalytic N-alkylation of amines with alcohols.[15] In both these cases[12,14,15] and in the majority of the Milstein-type systems,[16] the third donor of the pincer acts as a spectator, leading us to consider if simpler and largely unexplored bidentate pyridine-phosphaalkene ligands (**1**) in combination with a third exogenous ligand would behave in a similar fashion. Although it was synthesized concurrently with **E** in 1992,[10] no reports of cyclization of the Mes* group of parent pyridine-phosphaalkene (PN) **1a** (R′ = H) across its P═C double bond have been described (Chart 1).[17] In fact,

Chart 1. Previously Reported PNP Pincer E and PN Ligands 1a−c and Targeted 6-Substituted PN Ligands of Type 2

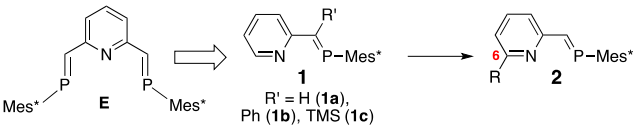

the coordination chemistry of **1a** in general has been scarcely reported with only a few examples, including a poorly characterized Cu(I) species.[10] Other C-functionalized analogues such as **1b** (R′ = Ph) can support square-planar Pt(II) and Pd(II) complexes, with the latter acting as a catalyst for the Overman−Claisen rearrangement.[18] A recent report by Ozawa also highlighted that **1b** could stabilize unusual Ni(I) species and highly distorted square-planar Ni(II) complexes and promote unusual P−C_{Ar} (C_{Ar} = Mes*) bond cleavage events,[19] all of which were hypothesized to originate from the presence of low-lying π^* orbitals on the P═C unit. Here, we report that the P═C double bond of pyridine-phosphaalkenes of type **2**, featuring sterically and electronically diverse substituents at the 6-position of the pyridine ring, is susceptible to C−H activation of the Mes* group and cyclization to a phospholane on coordination to Ru(II). Specifically, after preparing five PN ligands (**2a−e**) in an *E*-selective fashion via a phospha-Wittig methodology,[20] we discovered that, remarkably, on exposure to $RuCl_2(PPh_3)_3$ four distinct types of coordination complexes (**3−6**) are produced, three of which feature newly formed phospholane rings.

RESULTS AND DISCUSSION

Synthesis of Ligands of Type 2. Treatment of 6-substituted pyridine-2-carboxyaldehyde derivatives[21] with the phospha-Wittig[20] reagent Mes*P═PMe_3 resulted in the formation of PN ligands **2a−e** as yellow, crystalline solids in good yields (Scheme 3).[22]

Scheme 3. *E*-Selective Synthesis of 2a−e

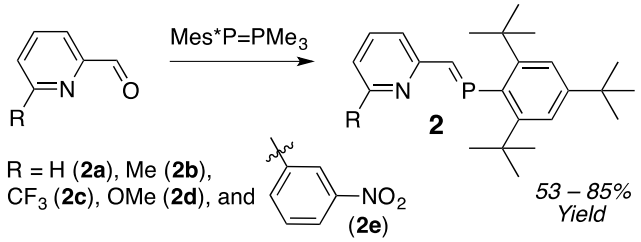

Their formation was identified by the diagnostic downfield shift of the P═C unit observed by $^{31}P\{^1H\}$ NMR spectroscopy, with the ^1H NMR spectra confirming that the phosphaalkenes were present in the *E* conformation (J_{PH} = 25 Hz).[21] Furthermore, the new PN ligands were characterized by $^{13}C\{^1H\}$ NMR spectroscopy, mass spectrometry, and elemental analysis. X-ray crystallography unequivocally established the structures of **2b,d,e** (Figures 1−3).

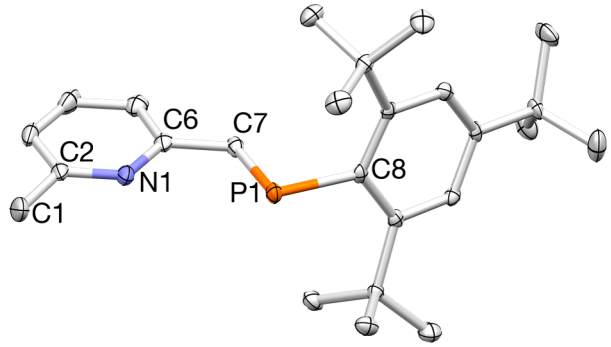

Figure 1. X-ray crystal structure of **2b**. Selected bond lengths (Å) and angles (deg) are shown in Table 1.

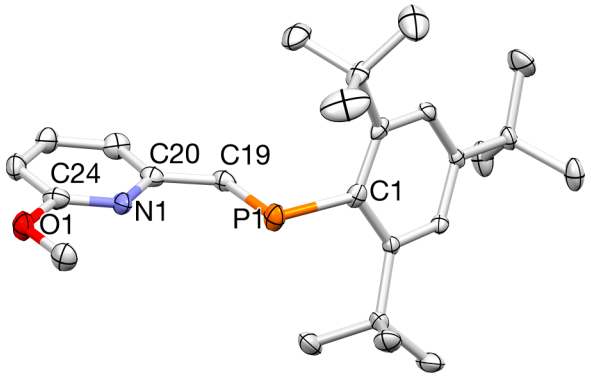

Figure 2. X-ray crystal structure of **2d**. Selected bond lengths (Å) and angles (deg) are shown in Table 1.

Solid-State Structures of 2. The solid-state structures of ligands **2a**,[22] and **2b,d,e** all feature P═C bond lengths (1.66−1.69 Å) within the normal range of other bidentate and pincer-type phosphaalkene-based ligands.[4a] Although the P−Mes* bond lengths show little variation (1.85−1.87 Å), they are marginally longer than most other phosphaalkene−aryl single bonds,[23,24] while their C═P−C bond angles are approximately 98°, consistent with a lack of hybridization at P.[4a] Other bond

DOI: 10.1021/acs.organomet.9b00425
Organometallics 2019, 38, 3338−3348

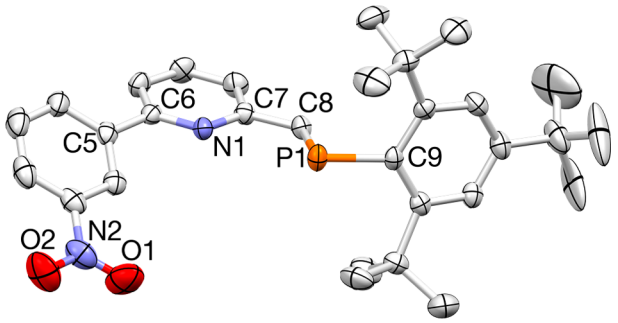

Figure 3. X-ray crystal structure of **2e**. Selected bond lengths (Å) and angles (deg) are shown in Table 1.

Scheme 4. Synthesis of Ru(II) Complexes 3−6

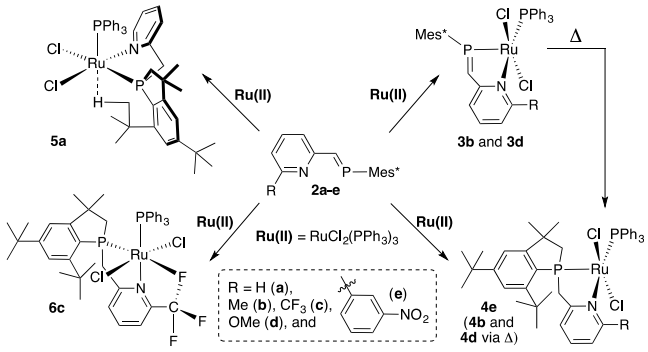

lengths and angles of interest are tallied in Table 1. In addition, the X-ray structures of **2b,d,e** (Figures 1−3) revealed that the *E* configuration of the P═C bond in combination with the two-carbon linker between the pyridine N atom and the P center create a promising binding pocket for a metal center.

Ru(II) Complexes. Treatment of **2a−e** with $RuCl_2(PPh_3)_3$ in benzene resulted in the formation of four distinct type of coordination complexes, pyridine-phosphaalkene-derived **3**, cyclized **4**, and six-coordinate **5** and **6**, all in reasonable yields (Scheme 4). The existence of the four different types of coordination complexes (**3−6**) was readily identified by NMR spectroscopy. Red solutions of **3b,d** showed that the phosphaalkene functionality remained intact, maintaining a significantly downfield shifted ^{31}P NMR signal (δ >290 ppm), which was coupled to the bound PPh_3 unit (**3b**, δ 36.0; **3d**, δ 34.0 ppm, J_{PP} = 36 Hz). On the other hand, a green solution of cyclized derivative **4e** featured an upfield-shifted ^{31}P NMR resonance (δ 90.3 ppm) reminiscent of other Ru-bound phospholanes,[25] also displaying coupling to PPh_3 (δ 48.6 ppm, J_{PP} = 36 Hz). A comparison of the $^{31}P\{^1H\}$ NMR spectra of **3b** and **4e** is shown in Figure 4. Moreover, the formation of the phospholane ring in **4e** generated a chiral P center, making the CH_2 protons of the new five-membered ring, the benzylic-type protons linking the pyridine to the phospholane unit, and the methyl groups on the phospholane diastereotopic, resulting in a series of ^1H NMR signals with complex splitting patterns integrating in a 1:1:1:1:3:3 ratio. Interestingly, prolonged heating of uncyclized **3b,d** in THF (>80 °C) resulted in smooth conversion to cyclized derivatives **4b,d** with the $^{31}P\{^1H\}$ (phospholane P atoms: **4b**, δ 91.1 ppm; **4d**, δ 89.9 ppm) and ^1H NMR spectra closely resembling that of **4e**. Both phosphaalkene-based **3b,d** and phospholane-derived **4b,d,e** were further characterized by $^{13}C\{^1H\}$ NMR spectroscopy, mass spectrometry, and elemental analysis. Ultimately, the solid-state structures of **3b** and **4b,e** were determined by X-ray crystallography (Figures 5−7).

Like **4b,d,e**, the $^{31}P\{^1H\}$ NMR spectrum of **5a** quickly established that the P═C functionality was no longer present. However, the two ^{31}P NMR signals detected were much different from those of cyclized **4b,d,e**, resonating at 64.0 and 66.8 ppm (J_{PP} = 39 Hz), suggesting that a different type of coordination complex was generated. Diastereotopic benzylic type protons were observed by ^1H NMR spectroscopy, confirming that C−H activation and cyclization had occurred, but one of the newly formed diastereotopic phospholane protons was drastically shifted upfield to 0.73 ppm. We hypothesized that the sterically diminutive C−H group of ligand **2a** created a coordination environment in which the phospholane, pyridine, and PPh_3 donors could all be mutually cis to one another. This would orient the strongly π donating chlorides trans to both the phospholane and pyridine, providing a rationale for the high-field PCH_2 signal and the unusual N-Ar resonance observed at 6.43 ppm. Recrystallization of **5a** from a concentrated THF solution exposed to pentane vapors afforded X-ray-quality crystals partially validating our hypothesis, but also establishing that **5a** was six-coordinate via an agostic interaction from one of the two remaining *t*-Bu groups (Figure 8). Evidence of this Ru−H−C interaction in solution, specifically an unusually upfield shifted *t*-Bu proton signal, was not observed.

Ru(II) complexes featuring agostic interactions are common,[26] normally resulting in five- or six-membered chelates. For example, Gusev synthesized Ru(II) dichloride **K** with one of the P-alkyl groups of the POP pincer utilizing an agostic interaction (Ru- - -H = 2.23 Å) to establish a five-membered ring,[27] while Shaw showed using azine phosphines in **L** that agostic interactions could be forced by placing the H atom in close proximity to the Ru center, affording six-membered rings (Figure 9, left).[28] Furthermore, Caulton[29] and Baratta (Ru- - -

Table 1. Selected Bond Lengths (Å) and Angles (deg) of Ligands 2a[22] and 2b,d,e[a]

	2a (R = H)[22]	**2b** (R = Me)	**2d** (R = OMe)	**2e** (R = Ar-*m* -NO_2)
P═C	1.663(3)	1.674(2)	1.694(4)	1.669(3)
P−Mes*	1.847(3)	1.8607(19)	1.873(3)	1.851(3)
C−P═C	99.15(14)	98.35(9)	98.27(16)	98.17(13)
N−C_{Ar}	1.39(5)	1.351(3)	1.368(4)	1.348(3)
N−C_{Ar}	1.31(5)	1.337(2)	1.319(5)	1.334(3)
C−N═C	119(4)	118.26(18)	116.4(3)	118.4(2)
backbone C−C	1.470(4)	1.466(3)	1.444(5)	1.461(4)
C_{Ar}−R	0.950	1.504(3)	1.364(4)	1.494(4)

[a]*R* factor (%): **2a** (6.0);[22] **2b** (4.73); **2d** (6.71); **2e** (4.50).

DOI: 10.1021/acs.organomet.9b00425
Organometallics 2019, 38, 3338−3348

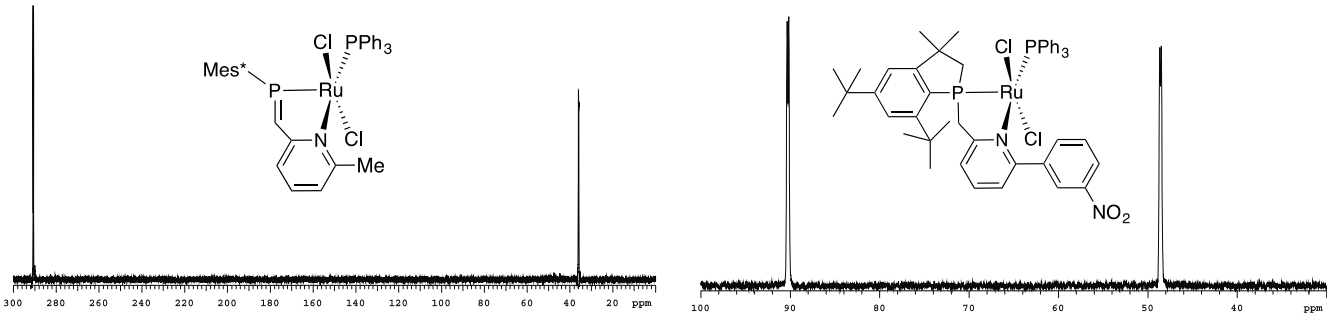

Figure 4. $^{31}P\{^{1}H\}$ NMR spectra (202 MHz, $CDCl_3$) of **3b** (left) and **4e** (right).

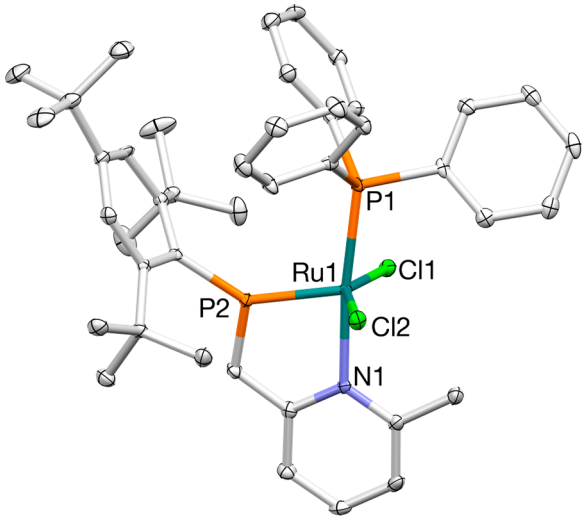

Figure 5. X-ray crystal structure of **3b** with the solvent molecule omitted for clarity. Selected bond lengths (Å) and angles (deg) are shown in Table 2.

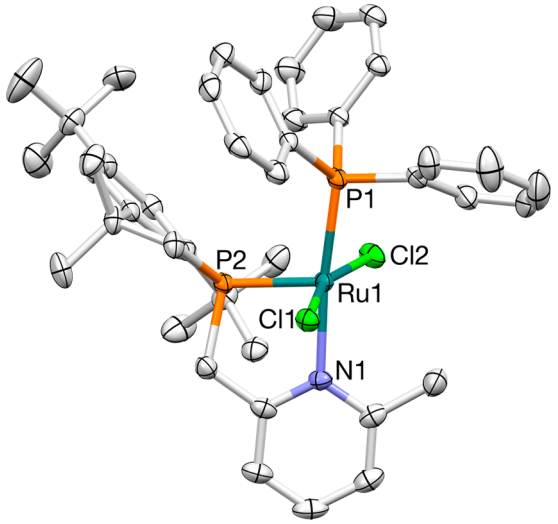

Figure 6. X-ray crystal structure of **4b**. Selected bond lengths (Å) and angles (deg) are shown in Table 2.

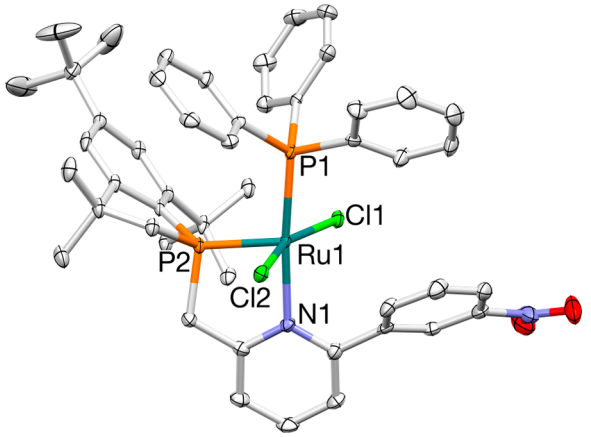

Figure 7. X-ray crystal structure of **4e**. Selected bond lengths (Å) and angles (deg) are shown in Table 2.

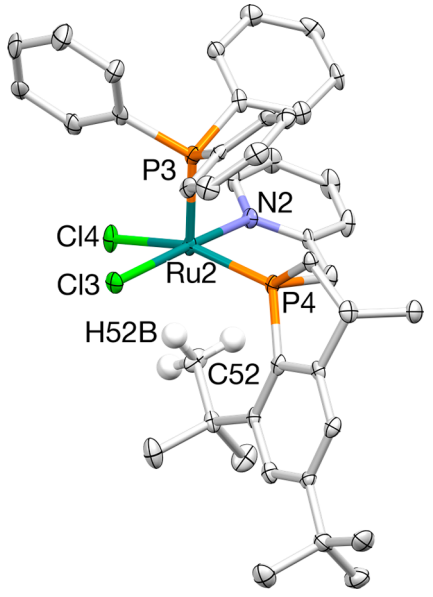

Figure 8. X-ray crystal structure of **5a**. Selected bond lengths (Å) and angles (deg) are shown in Table 2.

H = 2.185 and 2.198 Å)[30] demonstrated that double agostic interactions[31] could be formed by generating coordinatively unsaturated Ru(II) centers via halide abstraction or through the use of bulky phosphine ligands. Here, a seven-membered chelate to the Ru center was formed via a Ru−H contact of 2.069 Å with a Ru−H−C bond angle of 126.67° (Figure 9, right), both indicative of a bona fide agostic interaction (d(M−H) = 1.8−2.3 Å; M−H−C ≈ 90−140°).[32] A second-order perturbation theory analysis of the Fock matrix using NBO indicated that the three-center, two-electron Ru−H−C bond provided 11 kcal/mol of stabilization energy to **5a**. In all cases, these agostic interactions serve to coordinatively saturate the Ru(II) center, affording 18-electron complexes.

DOI: 10.1021/acs.organomet.9b00425
Organometallics 2019, 38, 3338−3348

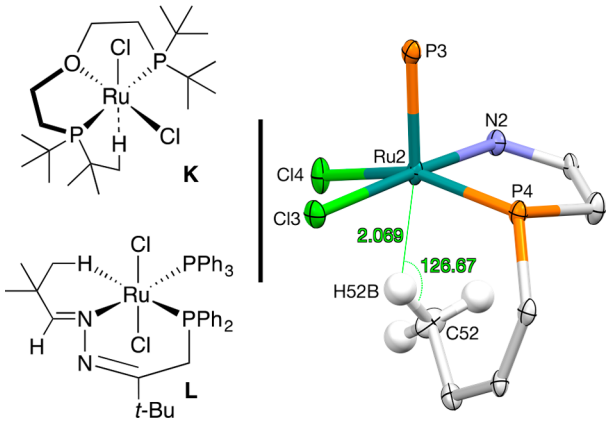

Figure 9. Structures of **K** and **L** (left) with trimmed X-ray crystal structure of **5a** showing the agostic interaction.

The other six-coordinate complex formed was **6c**, which is supported by CF_3-substituted ligand **2c**. Its NMR spectra closely mirrored **4b**,**d**,**e** with the exception that the ^{31}P NMR signal of the phospholane (δ 85.8 ppm) was not a doublet but rather an overlapping doublet of quartets with additional coupling to fluorine (J_{PP} = 40 Hz, J_{PF} = 20 Hz; Figure 10). This

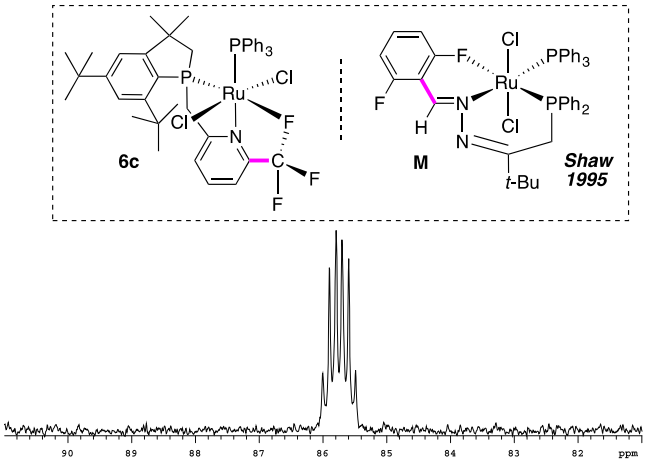

Figure 10. Enlarged $^{31}P\{^1H\}$ NMR spectrum (202 MHz, $CDCl_3$) of **6c** highlighting the overlapping doublet of quartets for the phospholane donor.

is due to interaction of the CF_3 unit with the 16-electron Ru center.[33] Shaw reported an analogous interaction in **M** with strikingly similar NMR spectra (structure shown in inset of Figure 10);[34] like **6c**, only the functionalized phosphine donor trans to F shows J_{PF} coupling (68 Hz). Interestingly, all three F atoms in **6c** and both F atoms in **M** are interacting with the Ru center on the NMR time scale, indicating that rotation about their sp^2–sp^3/sp^2 C–C bonds (shown in magenta in the inset of Figure 10) is facile and the Ru–F interaction is weak.[34]

In fact, by analogy to agostic (three-center, two-electron) versus anagostic (electrostatic) M–H–C bonds,[32] the reduced coupling constant in **6c** may reflect an anagostic/electrostatic Ru–CF_3 interaction, while the Ru–F "bond" in **M** is significantly more agostic. Distance is often the determining factor distinguishing agostic M–H–C interactions from anagostic interactions, with agostic interactions falling between 1.8 and 2.3 Å and anagostic interactions ranging from 2.3 to 2.9 Å.[32] Plenio has argued that for second- and third-row transition metals that a "true" M–F interaction must place the metal and fluorine atom within 3.0 Å of each other;[35] however, Togni has shown via a combination of NMR spectroscopy and X-ray crystallography that these interactions can persist above 3.0 Å.[36] Unfortunately, neither **6c** or **M** has been crystallographically characterized; thus, making an assignment of agostic versus anagostic based on distance is premature. However, the structure of **6c** was calculated at the B3LYP-D3/LACV3P** level, establishing the closest Ru- - -F contact at 2.978 Å (Figure 11). Although right on the 3 Å threshold,

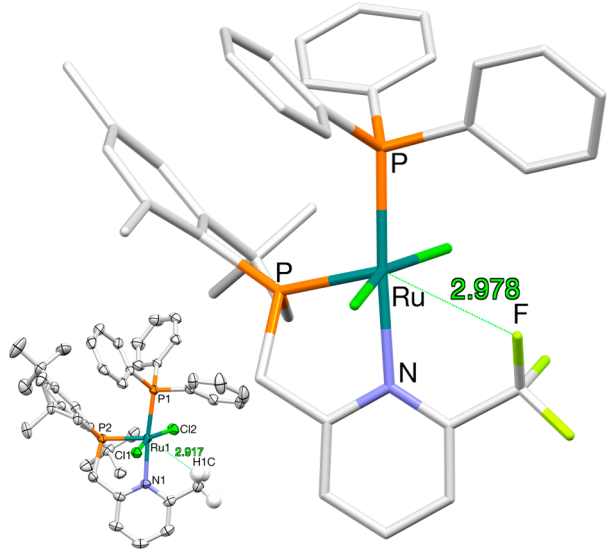

Figure 11. Computed structure of **6c** with comparison to **4b** (inset). The labels on the chloride donors were omitted, and the *t*-Bu groups were trimmed for clarity.

NBO calculations revealed that no bonding interaction could be found between the Ru center and the C–F bond or the F lone pairs, begging the question: is the "interaction" merely a geometric constraint? Reexamination of the structure of **4b** featuring the sterically similar methyl group suggests that this may be the case, as the nearest Ru- - -H contact sits at 2.917 Å (see inset, Figure 11). Furthermore, the broadened ^{31}P NMR signal of the phospholane in **4b** is likely due to a related dynamic process involving interaction of all three H atoms of the Me unit with the Ru center on the NMR time scale.

Solid-State Structures of Five-Coordinate Ru(II) Complexes. Complexes **3b** and **4b**,**e** all have distorted five-coordinate geometries skewed toward square pyramidal with narrow N–Ru–P bite angles.[37] The extremely small bite angle of the PN ligand in **3b** (80.23°) is likely the result of an abundance of short backbone bonds including the pyridine N–C bond, an sp^2–sp^2 C–C bond, and an intact P=C double bond, leading to a "tied-back" five-membered ring; a related square-planar Pd(Me)(Cl) complex supported by ligand **1c** (see Chart 1 for structure) also featured a N–Ru–P angle of approximately 80°.[22] Cyclization of the Mes* arm across the P=C bond in **4b**,**e** generates a new sp^3 benzylic-type carbon atom and a P–C single bond, providing more flexibility in the chelate and opening up the bite angle to almost 85°. As the bite angle increases, the phospholane unit shifts to a more "apical" position, and the overall geometries of the cyclized species are significantly closer to square pyramidal than is the case for uncyclized **3b**. A comparison of the bite angle and τ

DOI: 10.1021/acs.organomet.9b00425
Organometallics 2019, 38, 3338–3348

Table 2. Selected Bond Lengths (Å) and Angles (deg) of Ligands 3b, 4b,e, and 5a and Comparison with a Previously Reported[22] Pd Complex Supported by Ligand 1c (See Chart 1 for Structure of 1c)[a]

	[Pd(Me)(Cl)(1c)][b]	3b (R = Me)	4b (R = Me)	4e (R = Ar-*m*-NO_2)	5a (R = H)
N−Ru−$P_{P=C}$ (bite angle)[c]	79.45(10)	80.23(5)	84.43(7)	84.69(5)	84.11(14)
τ[38]	N/A	0.38	0.19	0.23	N/A
P−$C_{PN\text{-}Chelate}$	1.674(4)	1.671(3)	1.838(3)	1.853(2)	1.847(7)
P−Mes*	1.808(4)	1.825(2)	1.863(3)	1.860(2)	1.835(7)
Ru−$P_{P=C}$[c]	2.1744(14)	2.1498(6)	2.1826(9)	2.2007(6)	2.2436(17)
Ru−P_{PPh3}	N/A	2.3382(7)	2.2986(9)	2.3072(6)	2.2447(19)
C−P=C[c]	114.26(19)	116.48(11)	110.42(14), 105.29(14), 92.94(14)	111.30(10), 103.23(11), 92.75(10)	105.8(3), 101.9(3), 91.9(3)
Ru−N_{py}	2.164(4)	2.147(2)	2.145(2)	2.1608(19)	2.103(5)

[a] *R* factor (%): [Pd(Me)(Cl)(**1c**)] (5.14);[22] **3b** (3.93); **4b** (3.75); **4e** (4.12); **5a** (5.78). [b] The bond lengths and angles given in this column are for a Pd complex, not Ru. [c] For complexes **4b,e** and **5a**, cyclization converted the P=C bond into a P−C bond, and therefore, the P atom indicated is for the newly formed phospholane P.

values[38] (τ = 1 = idealized TBP; τ = 0 = idealized square pyramidal) is shown in Table 2.

In addition, the X-ray structure determination of the methyl series, specifically, **2b** (see Table 1 for structural data), **3b**, and **4b** provided valuable insight into the structural changes of the phosphaalkene functionality upon binding and cyclization. At first glance, the most striking observation is that the P=C bond length does not change on coordination to the Ru(II) center (**2b** vs **3b**). Phosphaalkenes are strong π acceptors;[4a] thus, the bond is expected to elongate. However, on complexation to metals, the P center undergoes extensive rehybridization from largely unhybridized (high s character in lone pair/high p character in P−C bonds) toward sp^2, adding s character to the P−C bonds and resulting in their contraction; the two opposing effects cancel each other out, yielding no overall change in the P=C bond length.[39] Further evidence to support this rehybridization is observed in the shortening of the P−Mes* bond and widening of the C−P=C bond angle to 116.48(11)°; NBO calculations corroborate these findings (Table 3). Addition of the C−H bond on the Mes* arm across the P=C bond also has profound consequences (**3b** → **4b**, Table 2). Most obvious is the drastic elongation of the P−C bond as it is transformed from a three-coordinate, P=C double bond into a four-coordinate, P−C single bond, but the P−Mes* bond also lengthens. Likewise, these observations can be rationalized by invoking hybridization arguments. The P donor in the pyridine-phosphaalkene ligand is ~sp^2 (C−P=C bond angle = 116.48°), while the phospholane functionality adopts nearly sp^3 hybridization. The added p character in the P−C bonds leads to their elongation, while the P center simultaneously reorganizes to a more tetrahedral geometry (average C−P−C bond angle = 102.9°).[40] A final more subtle observation is that the Ru−P bond to the new PN ligands are all shorter than that to PPh_3. Again, the sp^2-hybridized P atom in the pyridine-phosphaalkene should afford the shortest Ru−P bond (which it does), but why is the Ru−P bond length to the phospholane shorter than that to PPh_3? Recent reports by Glueck[41] and Higham[42] have compared phosphine and phosphirane donors, finding that when they are of similar size, phosphiranes feature shorter M−P bonds (M = Pt, Rh, Au) because of increased s character in the P lone pair enforced by the severely acute angles of the three-membered ring. We expected similar arguments could be made for the phospholane donor; however, DFT calculations revealed that Ru−$P_{phospholane}$ and Ru−PPh_3 bonds contained the same amount of s character (33% s, Table 3). Instead, we speculate that the shorter Ru−$P_{phospholane}$ bond is due to the fact that the trans coordination site is vacant. Without a trans ligand, the Ru center and phospholane P maximize their orbital overlap, resulting in a shorter Ru−P bond relative to the PPh_3 unit, which has to compete with the pyridine donor for electron density.[43,44]

Table 3. Selected Atom Hybridization of Ligand 2b, Its Cyclized Counterpart (Unbound to a Metal Center), and Ru(II) Complexes 3b and 4b

	2b	free phospholane	3b	4b
P LP or P−Ru bond	$sp^{0.51}$	$sp^{0.80}$	$sp^{1.51}$	$sp^{2.02}$
P−C_{Mes*} bond	$sp^{5.95}$	$sp^{5.30}$	$sp^{2.37}$	$sp^{3.16}$
P=C or P−CH_2 linker	$sp^{3.86}$	$sp^{6.15}$	$sp^{2.17}$	$sp^{3.68}$
Ph_3P−Ru bond	N/A	N/A	$sp^{2.04}$	$sp^{1.98}$

Solid-State Structure of Six-Coordinate 5a. Ru(II) complex **5a** adopts a distorted-octahedral geometry featuring cis-oriented chlorides in plane with the PN chelate; the PPh_3 ligand is bound in the "apical" position and the agostic Ru−H−C interaction is located trans to it, residing in the sixth coordination site. This is in contrast to **3b** and **4b,e**, in which the chlorides and PPh_3/pyridine donors are mutually trans to one another with the phosphaalkene-derived P atom occupying the apical site in the square pyramid (Chart 2). This different spatial arrangement of ligands at Ru(II) has subtle structural consequences that are a manifestation of the trans influence.[43] For example, the Ru−$N_{pyridine}$ bond (Ru−N_{avg} = 2.151 Å) in **3b** and **4b,e** is approximately 0.05 Å longer than in **5a** (Ru−N = 2.103(5) Å), and the longest Ru−Cl bond (2.4612(16) Å) by roughly 0.06 Å (Ru−Cl = 2.4016(6) Å in **4e**) is found trans to the phospholane in **5a**; both observations are consistent with the pronounced trans influence of a PR_3 group relative to a chloride or pyridine donor.[44]

Chart 2. Comparison of the Spatial Arrangement of Donor Atoms to the Ru Center in 3b and 4b,e versus 5a

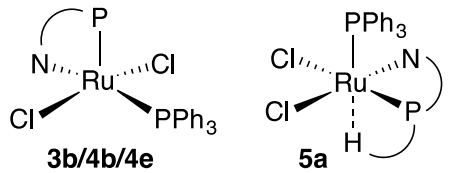

DOI: 10.1021/acs.organomet.9b00425
Organometallics 2019, 38, 3338−3348

On the other hand, the most significant structural effect on going from five-coordinate **3b** and **4b,e** to six-coordinate **5a** is the drastic pyramidalization of the phospholane center with the sum of the C−P−C angles totaling less than 300° (Table 2, above).[45] This may be rooted in geometric constraints involved in the fact that the P atom is incorporated into a few unusual ring structures, including a fused 5,7-system with a Ru/P ring junction and a phosphindoline,[46] which is formally annulated to a seven-membered ring through formation of the Ru−H−C agostic bond. This agostic interaction may also contribute to the pyramidalization of the phospholane, as the PN chelate is now "tridentate"[47] and bound in a facial arrangement,[48] enforcing bite angles at Ru to approach 90°.

Origin of Cyclization of Phosphaalkene to Phospholane at Ru. The presence of an agostic interaction also has mechanistic implications, because substrate binding is the first step in activation at a transition-metal center.[49] With PN ligands **2a−e**, there is a clear electronic component to whether or not the *t*-Bu unit of the Mes* group is activated and added across the P═C bond. Electron-rich ligands **2b,d** formed **3b,d** (R = Me, OMe), in which the phosphaalkene unit persisted (unless heated in THF), while the more electron poor ligands **2c,e** (R = CF_3, Ar-*m*-NO_2) including parent **2a** underwent cyclization affording TM complexes **6c**, **4e**, and **5a** featuring a modified PN ligand containing a new phospholane donor.

Literature Precedent. Two relevant mechanisms resulting in the cyclization of the Mes* group across a P═C unit to give phospholanes have been previously reported (Scheme 5). The

Scheme 5. Previously Proposed Mechanisms of Cyclization of the P−Mes* Group across the P═C Double Bond

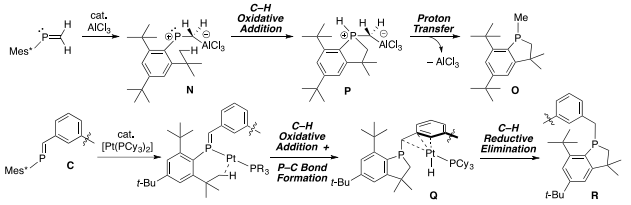

first was a Lewis acid catalyzed approach experimentally demonstrated by exposing Mes*P═CH_2 to $AlCl_3$.[50] The reaction generated phosphenium (PR_2^+) intermediate **N**, which C−H activated the *t*-Bu group of the Mes* arm, affording P−Me phospholane **O** after proton transfer from zwitterionic **P**.[50,51] The second mechanism, based on reactivity observed with **C** (vide supra) and supported largely by computations (B3PW91 functional with 6-31G* basis set for H, C, and P atoms and LANL2TZ(f) basis set for Pt), involved coordination of the phosphaalkene to a phosphine-ligated Pt(0) catalyst followed by stepwise C−H oxidative addition of the *t*-Bu group, intramolecular P−C bond formation to give η^3 intermediate **Q**, and C−H reductive elimination of phospholane **R**.[7]

We envisioned that either mechanism could be operative here. For example, if the Ru(II) center acts purely as a Lewis acid (M^+, no redox chemistry), complexation of the nitrogen atom to Ru(II) opens up a pathway for dearomatization of the pyridine moiety and generation of reactive phosphenium intermediate **S** (Scheme 6, right). Addition of the C−H bond[50,51] across the cationic P center in **S** constructs a phospholane ring; subsequent proton transfer and rearomatization results in the formation of the new pyridine-

Scheme 6. Two Potential Mechanisms of Cyclization of the P−Mes* Group across Its P═C Double Bond in Ligands 2a−e on Exposure to a Ru(II) Center

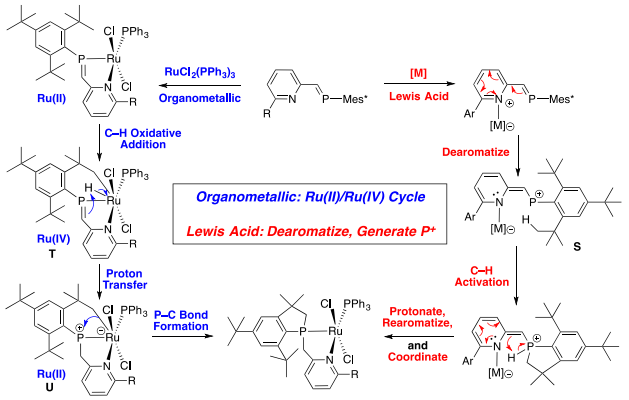

phospholane ligand, which coordinates to the Ru(II) center in a bidentate fashion. On the other hand, initial coordination of the pyridine-phosphaalkene to the Ru(II) center could promote oxidative addition of the *t*-Bu group, giving the 7-coordinate, 18-electron Ru(IV) complex **T** (Scheme 6, left).[52] Proton transfer to the phosphaalkene carbon atom will furnish zwitterionic **U**, featuring a cationic phosphorus donor. Intramolecular nucleophilic attack of the alkyl arm on the phosphorus atom will quench the charges on both Ru and P and simultaneously give the phospholane ring. These mechanistic possibilities will be explored from both a computational and experimental standpoint in the future.

CONCLUSIONS AND OUTLOOK

Like their pincer counterparts (**C** and **E**), simple, bidentate pyridine-phosphaalkene (PN) ligands **2a−e** are capable of cyclizing at transition-metal centers. Unexpectedly, four distinct types of transition metal complexes (**3−6**) are produced on exposure of these five ligands (**2a−e**), varying only in their 6-substituent to $RuCl_2(PPh_3)_3$. Complexes **4−6** feature a new phospholane donor tethered to a pyridine ring via a CH_2 spacer; future studies will assess if these acidic, benzylic-type protons can be deprotonated to generate dearomatized complexes such as **7** (Scheme 7, shown using

Scheme 7. Future Dearomatization Studies

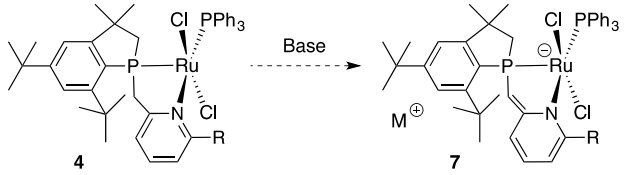

4 as a representative example). Analogous complexes supported by pincer ligands have promoted numerous forms of strong bond activation (C−H,[53] N−H,[12,54] O−H,[55] etc.) and dehydrogenation-based catalytic processes.[16] We will target energy relevant substrates with the secondary goal of developing enantioselective catalytic reactions utilizing the phospholane P as the source of chirality, a monodentate chiral phosphine in place of PPh_3, or a pyridine featuring an asymmetric R group.

DOI: 10.1021/acs.organomet.9b00425
Organometallics 2019, 38, 3338−3348

EXPERIMENTAL SECTION

General Experimental Details. Unless otherwise specified, all reactions and manipulations were performed under a nitrogen atmosphere in a MBraun glovebox or using standard Schlenk techniques. All glassware was oven-dried overnight (at minimum) at 140 °C prior to use. Anhydrous solvents were purchased directly from chemical suppliers (Aldrich or Acros), pumped directly into the glovebox, and stored over oven-activated 4 or 5 Å molecular sieves (Aldrich). $RuCl_2(PPh_3)_3$ and Zn dust were purchased from Strem and used as is; PMe_3 was also bought from Strem and stored over molecular sieves prior to use. The 6-substituted pyridine-2-carboxyaldehyde derivatives were obtained from Sigma-Aldrich, and Mes*PCl_2 was prepared via a literature protocol.[56] NMR spectra were obtained on Varian spectrometers operating at 300, 400, or 500 MHz; all spectra are displayed in the Supporting Information. NMR chemical shifts are reported as ppm relative to tetramethylsilane and are referenced to the residual proton or ^{13}C signal of the solvent (^1H $CDCl_3$, 7.27 ppm; ^1H C_6D_6, 7.16 ppm; ^{13}C $CDCl_3$, 77.16 ppm; ^{13}C C_6D_6, 128.06 ppm). Mass spectroscopic data were collected on an Agilent 6545 Accurate-Mass Q-TOF LC/MS instrument (NSF CHE-1532310). Analytical data were obtained from the CENTC Elemental Analysis Facility at the University of Rochester, funded by NSF CHE-065-456. All X-ray-quality crystals were analyzed at the Small Molecular X-ray Crystallography Facility located at the University of California, San Diego.

Synthesis of Pyridine-Phosphaalkenes of Type 2. Derivative **2a** was previously prepared as an *E*/*Z* mixture by Geoffroy[10] and selectively (at low temperature) as the *E* isomer by Bickelhaupt[22] using a phospha-Peterson methodology.[17] Its full spectroscopic characterization is reported in ref 22. Using a phospha-Wittig methodology, in a manner as described below for **2b**, parent **2a** was isolated in 83% yield.

***E*-Selective Synthesis of 2b using a Phospha-Wittig Methodology.** Mes*PCl_2 (1.00 g, 2.88 mmol) and Zn dust (940 mg, 14.4 mmol, 5 equiv) were combined in a vial, and 4 mL of THF was added. Treatment of the suspension with a room-temperature solution of PMe_3 (560 mg, 7.36 mmol, 2.6 equiv) in THF resulted in a yellow reaction mixture. The reaction mixture was stirred at room temperature for 1 h and filtered through a Celite plug directly into a solution of 6-methylpyridine-2-carboxaldehyde (262 mg, 2.16 mmol, 0.75 equiv) in 3 mL of THF to afford a homogeneous yellow-orange solution. After it was stirred for 10 min, the reaction mixture was concentrated under vacuum. The yellow residue was extracted with 5 mL of pentane and filtered through a Celite plug. The filtrate was concentrated under vacuum and recrystallized from 5 mL of a 50/50 solution of THF and acetonitrile at −35 °C to give a yellow solid (700 mg, 1.84 mmol, 85% yield).

Anal. Calcd for $C_{25}H_{36}NP$: C, 78.70; H, 9.51; N, 3.67. Found: C, 78.42; H, 9.54; N, 3.59. HRMS: *m*/*z* calcd for $C_{25}H_{36}NP$ $[M]^+$, 381.2585; found, 381.2591. $^{31}P\{^1H\}$ NMR ($CDCl_3$): δ 280.4. ^1H NMR ($CDCl_3$): δ 8.10 (d, *J* = 25.0 Hz, 1H, P═CH), 7.51 (m, 2H, Ar), 7.43 (s, 2H, Ar), 6.97 (br m, 1H, Ar), 2.53 (s, 3H, Me), 1.52 (s, 18H, *t*-Bu), 1.35 (s, 9H, *t*-Bu). $^{13}C\{^1H\}$ NMR ($CDCl_3$): δ 175.6 (d, *J* = 33.8, P═C), 158.2 (Ar), 157.5 (d, *J* = 15.0 Hz, Ar), 153.9 (Ar), 149.7 (Ar), 148.5 (Ar), 139.0 (d, *J* = 52.5 Hz, Ar), 136.4 (Ar), 123.7 (Ar), 121.6 (Ar), 119.4 (Ar), 117.0 (d, *J* = 20.0 Hz, Ar), 38.2 (CMe_3), 34.0 (*t*-Bu), 33.9 (*t*-Bu), 31.8 (CMe_3), 31.6 (CMe_3), 31.4 (*t*-Bu), 30.9 (Me).

Ligands **2c**−**e** were prepared in an analogous fashion to **2b** using a phospha-Wittig methodology. Full experimental details are included in the Supporting Information.

Syntheses of Ru(II) Complexes 3−**6.** *Pyridine-Phosphaalkene Complex **3b**.* $RuCl_2(PPh_3)_3$ (126 mg, 0.131 mmol) was loaded into a vial and treated with a solution of **2b** (50 mg, 0.131 mmol) in 1 mL of benzene at room temperature. The dark reaction mixture was transferred to a J. Young tube and monitored by $^{31}P\{^1H\}$ NMR spectroscopy. After it was heated at 60 °C for 120 h, the solution turned dark red, and the $^{31}P\{^1H\}$ NMR spectrum showed two doublets at 290.7 and 36.0 ppm. The mixture was subsequently filtered through Celite, and the filtrate was concentrated under vacuum. The crude dark red solid was recrystallized from toluene layered with pentane at −35 °C (83 mg, 0.102 mmol, 78% yield). Crystals suitable for X-ray crystallography were collected by slow diffusion of pentane vapors into a concentrated toluene solution.

Anal. Calcd for $C_{47}H_{59}Cl_2NOP_2Ru$ [M + THF]: C, 63.58; H, 6.70; N, 1.58. Found: C, 63.24; H, 6.85; N, 1.46. HRMS: *m*/*z* calcd for $C_{48}H_{51}N_2O_2P_2Ru$ $[M]^+$, 815.1917; found, 815.2510. $^{31}P\{^1H\}$ NMR ($CDCl_3$): δ 290.7 (d, *J* = 36.4, C═P), 36.0 (d, *J* = 36.4, PPh_3). ^1H NMR ($CDCl_3$): δ 7.56 (t, *J* = 8.0 Hz, 1H, Ar), 7.46−7.39 (m, 8H, Ar), 7.38−7.32 (m, 3H, Ar), 7.26−7.22 (m, 6H, Ar), 6.92 (d, *J* = 7.5 Hz, 1H, Ar), 6.54 (d, *J* = 4.1 Hz, 1H, Ar), 2.85 (s, 3H, Me), 1.33 (s, 9H, *t*-Bu), 1.23 (s, 18H, *t*-Bu).$^{13}C\{^1H\}$ NMR (125 MHz, $CDCl_3$): δ 163.3 (Ar), 159.5 (Ar), 155.2 (Ar), 153.4 (Ar), 136.0 (Ar), 134.7 (d, *J* = 10.0 Hz, Ar), 133.2 (Ar), 132.9 (Ar), 129.5 (Ar), 127.8 (d, *J* = 10.0 Hz, Ar), 125.6 (d, *J* = 26.0 Hz, Ar), 123.8 (d, *J* = 10.0 Hz, Ar), 119.2 (d, *J* = 25.0 Hz, C═P), 119.0 (Ar), 39.8 (CMe_3), 35.2 (CMe_3), 33.9 (*t*-Bu), 31.0 (*t*-Bu), 24.7 (Me).

Due to its similarity to that for **3b**, the synthesis of **3d** is included in the Supporting Information.

*Cyclized (Pyridine-Phospholane) Complex **4b**.* A solution of **3b** (15 mg, 0.019 mmol) in 1 mL of THF was heated at 80 °C for 48 h, at which time the phosphaalkene resonance was no longer observed by ^{31}P NMR spectroscopy. The cyclized complex (^{31}P NMR: δ 91.1, 46.7) was filtered through a pad of Celite, and the filtrate was concentrated under vacuum. The crude solid was recrystallized from a 1/3 solution of THF/pentane at −35 °C to give dark green crystals (12 mg, 0.015 mmol, 80% yield). Crystals suitable for X-ray crystallography were collected by slow diffusion of pentane vapors into a concentrated THF solution.

HRMS: *m*/*z* calcd for $C_{45}H_{54}ClN_2P_2Ru$ [M − (Cl^-) + $NCMe]^+$, 821.2494; found, 821.2516. $^{31}P\{^1H\}$ NMR (202 MHz, $CDCl_3$): δ 91.1 (br, CH_2P), 48.7 (d, *J* = 36.4 Hz, PPh_3). ^1H NMR (500 MHz, $CDCl_3$): δ 7.61−7.56 (m, 2H, Ar), 7.40 (t, *J* = 9.0 Hz, 6H, Ar), 7.31 (t, *J* = 8.5 Hz, 4H, Ar), 7.21−7.14 (m, 7H, Ar), 6.96 (d, *J* = 1.5 Hz, 1H, Ar), 4.23 (dd, *J* = 17.0, 11.0 Hz, 1H, benzylic N_{Ar}), 3.99 (dd, *J* = 17.0, 10.0 Hz, 1H, benzylic N_{Ar}), 2.80 (s, 3H, Me), 2.17−1.96 (m, 2H, CH_2P), 1.38 (s, 9H, *t*-Bu), 1.23 (s, 9H, *t*-Bu), 1.10 (s, 3H, CMe_2), 0.79 (s, 3H, CMe_2). $^{13}C\{^1H\}$ NMR (125 MHz, $CDCl_3$): δ 162.1 (Ar), 160.4 (Ar), 157.3 (d, *J* = 21.3, Ar), 156.7 (d, *J* = 7.5 Hz, Ar), 153.6 (Ar), 136.2 (Ar), 134.6 (d *J* = 10.0 Hz, Ar), 133.7 (d, *J* = 42.5 Hz, Ar), 129.3 (Ar), 129.0 (Ar), 128.3 (d, *J* = 12.5 Hz, Ar), 127.9 (d, *J* = 8.8 Hz, Ar), 126.8 (d, *J* = 10.0 Hz, Ar), 123.8 (Ar), 119.2 (d, *J* = 10.0 Hz, Ar), 117.9 (d, *J* = 10.0 Hz, Ar), 50.9 (d, *J* = 22.5 Hz, benzylic), 47.6 (d, *J* = 43.8 Hz, PCH_2CMe_2), 43.2 (CMe_2), 37.9 (CMe_3), 35.4 (*t*-Bu), 35.0 (CMe_3), 34.1 (*t*-Bu), 31.3 (*t*-Bu), 28.6 (d, *J* = 10.0 Hz, CMe_2), 25.0 (Me).

The closely related thermally induced cyclization of **3d** to **4d** can be found in the Supporting Information.

*Cyclization of **2e** to **4e**.* $RuCl_2(PPh_3)_3$ (197 mg, 0.205 mmol) was loaded into a vial and treated with a solution of **2e** (100 mg, 0.205 mmol) in 2 mL of benzene at room temperature. The dark reaction mixture was transferred to a J. Young tube and monitored by $^{31}P\{^1H\}$ NMR spectroscopy. After it was heated at 80 °C for 72 h, the reaction mixture turned dark green, and the $^{31}P\{^1H\}$ NMR spectrum showed two doublets at 90.3 and 48.6 ppm. The mixture was subsequently filtered through Celite, and the filtrate was concentrated under vacuum. The dark green residue was recrystallized from a 5 mL solution of THF layered with pentane at −35 °C (185 mg, 0.201 mmol, 98% yield). Crystals suitable for X-ray crystallography were collected by slow diffusion of pentane vapors into a concentrated THF solution.

Anal. Calcd for $C_{48}H_{52}Cl_2N_2O_2P_2Ru$ was consistently low (three attempts) in carbon, for example: C, 62.47; H, 5.68; N, 3.04. Found: C, 61.83; H, 5.69; N, 2.69. HRMS: *m*/*z* calcd for $C_{48}H_{52}Cl_2N_2O_2P_2Ru$ $[M]^+$, 922.1925; found, 922.1906. $^{31}P\{^1H\}$ NMR ($CDCl_3$): δ 90.3 (d, *J* = 36.4 Hz, P-Mes*), 48.6 (d, *J* = 36.4 Hz, PPh_3). ^1H NMR ($CDCl_3$): δ 8.57 (s, 1H, Ar), 8.11 (d, *J* = 7.0 Hz, 1H, Ar), 8.03 (d, *J* = 9.5 Hz, 1H, Ar), 7.87 (t, *J* = 8.0 Hz, 1H, Ar), 7.58−7.54 (m, 3H, Ar), 7.27 (m, *J* = 7.0 Hz, 9H, Ar), 7.08 (t, *J* = 6.5 Hz, 6H, Ar), 6.95 (s, 1H, Mes*), 6.89 (t, *J* = 8.0 Hz, 1H, Ar), 4.25

DOI: 10.1021/acs.organomet.9b00425
Organometallics 2019, 38, 3338−3348

(overlapping m, J = 16.5, 10 Hz, 2H, PCH_2N), 2.34 (dd, J = 16.5, 5.0 Hz, 1H, PCH_2), 1.90−1.81 (m, 1H, PCH_2), 1.35 (s, 9H, t-Bu), 1.15 (s, 9H, t-Bu), 1.12 (s, 3H, C(Me)$_2$), 0.78 (s, 3H. C(Me)$_2$). ^{13}C{^{1}H} NMR (125 MHz, $CDCl_3$): δ 164.1 (Ar), 160.8 (Ar), 157.5 (d, J = 21.3 Hz, Ar), 156.6 (d, J = 7.5 Hz, Ar), 153.7 (Ar), 148.8 (Ar), 142.6 (Ar), 136.8 (Ar), 134.9 (d, J = 8.8 Hz, Ar), 133.8 (d, J = 42.5 Hz, Ar), 131.9 (Ar), 131.4 (Ar), 129.2 (Ar), 127.6 (d, J = 10.0 Hz, Ar), 126.8 (d, J = 10.0 Hz, Ar), 126.4 (Ar), 123.9 (Ar), 123.8 (Ar), 123.2 (Ar), 121.6 (d, J = 10.0 Hz, Ar), 118.1 (d, J = 10.0 Hz, Ar), 50.9 (d, J = 22.5 Hz, benzylic), 45.9 (d, J = 42.5 Hz, Phospholane PCH_2), 42.7 (CMe_2), 37.7 (CMe_3), 35.3 (CMe_2), 35.0 (CMe_3), 34.0 (t-Bu), 31.0 (t-Bu), 28.8 (d, J = 10 Hz, CMe_2).

Six-Coordinate ***5a*** *(C−H Agostic Complex).* $RuCl_2(PPh_3)_3$ (55 mg, 0.149 mmol, 1.0 equiv) was loaded into a vial and treated with a solution of **2a** (144 mg, 0.149 mmol, 1.0 equiv) in 1 mL of benzene at room temperature. The dark reaction mixture was transferred to a J. Young tube and monitored by ^{31}P{^{1}H} NMR spectroscopy. After it was heated at 80 °C for 72 h, the solution turned dark red, and the ^{31}P{^{1}H} NMR spectrum showed two doublets at 66.8 and 64.0 ppm. The mixture was subsequently filtered through a Celite plug using Et_2O, and the filtrate was concentrated under vacuum. The crude product was recrystallized from a concentrated solution of benzene at 25 °C to give a red solid (50 mg, 0.062 mmol, 42% yield). Crystals suitable for X-ray crystallography were collected by slow diffusion of pentane vapors into a concentrated THF solution.

Anal. Calcd for $C_{42}H_{49}Cl_2NP_2Ru$: C, 62.92; H, 6.16; N, 1.75. Found: C, 63.31; H, 6.12; N, 1.37. HRMS: m/z calcd for $C_{42}H_{49}ClNP_2Ru^+$ [M − (Cl$^-$)]$^+$, 766.2067; found, 766.2077. ^{31}P{^{1}H} NMR (202 MHz, $CDCl_3$): δ 66.8 (d, J = 39.3 Hz, PPh_3), 64.0 (d, J = 39.3 Hz, CH_2P). ^{1}H NMR (500 MHz, $CDCl_3$): δ 9.31 (dd, J = 6.1, 1.8 Hz, 1H, Ar), 7.76−7.82 (m, 5H, Ar), 7.42 (dd, J = 4.8, 1.8 Hz, 1H, Ar), 7.27−7.20 (m, 5H, Ar), 7.19−7.13 (m, 6H, Ar), 7.10 (d, J = 1.8 Hz, 1H, Mes*), 7.04 (d, J = 7.1 Hz, 1H, Ar), 6.43 (t, J = 7.1 Hz, 1H, Ar), 3.69 (dd, J = 18.4, 11.4 Hz, 1H, CH_2Ar), 3.44 (dd, J = 18.4, 8.5 Hz, 1H, CH_2Ar), 2.22 (dd, J = 15.3, 7.8 Hz, 1H, PCH_2), 1.30 (s, 9H, t-Bu), 1.26 (s, 3H, Me), 1.25 (s, 3H, Me), 0.86 (d, J = 1.6 Hz, 9H, t-Bu), 0.73 (dd, J = 15.2, 2.2 Hz, 1H, PCH_2). ^{13}C{^{1}H} NMR (125 MHz, $CDCl_3$): δ 164.7 (Ar), 157.0 (Ar), 156.2 (d, J = 14.2 Hz, Ar), 154.2 (Ar), 152.2 (d, J = 10.6 Hz, Ar), 134.8 (d, J = 22.3 Hz, Ar), 134.6 (Ar), 133.9 (d, J = 9.5 Hz, Ar), 129.0 (Ar), 127.6 (d, J = 10.1 Hz, Ar), 124.6 (d, J = 8.2 Hz, Ar), 121.9 (Ar), 121.7 (d, J = 11.4 Hz, Ar), 118.8 (d, J = 8.2 Hz, Ar), 46.8 (d, J = 20.0 Hz, CH_2Ar), 43.6 (d, J = 5.5 Hz, CMe_2), 39.4 (d, J = 31.3 Hz, PCH_2), 35.0 (CMe_3), 30.4 (CMe_3), 32.8 (t-Bu), 31.7 (d, J = 9.6 Hz, CMe_2), 31.2 (t-Bu), 30.5 (d, J = 5.3 Hz, CMe_2).

Six-Coordinate ***6c*** *("C−F Agostic" Complex).* $RuCl_2(PPh_3)_3$ (128 mg, 0.130 mmol) was loaded into a vial and treated with a solution of **2c** (60 mg, 0.130 mmol) in 2 mL of benzene at room temperature. The dark reaction mixture was transferred to a J. Young tube and monitored by ^{31}P{^{1}H} NMR spectroscopy. After it was heated at 60 °C for 240 h, the solution turned dark green, and the ^{31}P{^{1}H} NMR spectrum showed two doublets at 85.8 and 50.2 ppm. The mixture was subsequently filtered through Celite, and the filtrate was concentrated under vacuum. The crude residue was recrystallized from THF layered with Et_2O at −35 °C to give green crystals (35 mg, 0.039 mmol, 30% yield).

^{31}P NMR ($CDCl_3$): δ 85.8 (overlapping dq, J = 42.8, 21.5 Hz, CH_2P) 50.2 (d, J = 42.8 Hz, PPh_3). ^{1}H NMR ($CDCl_3$): δ 7.89 (t, J = 7.8 Hz, 1H, Ar), 7.72 (d, J = 7.8 Hz, 1H, Ar), 7.68 (d, J = 7.8 Hz, 1H, Ar), 7.60 (dd, J = 4.6, 2.0 Hz, 1H, Ar), 7.40 (t, J = 7.8 Hz, 4H, Ar), 7.30 (m, 2H, Ar), 7.17 (m, 7H, Ar), 6.97 (d, J = 2.0 Hz, 1H, Ar), 4.33 (dd, J = 16.7, 10.7 Hz, 1H, CH_2Ar), 4.18 (dd, J = 16.7, 9.8 Hz, 1H, CH_2Ar), 2.27 (dd, J = 16.4, 5.1 Hz, 1H, CH_2P), 1.99 (dd, J = 16.4, 10.7 Hz, 1H, CH_2P), 1.38 (s, 9H, t-Bu), 1.22 (s, 9H, t-Bu), 1.10 (s, 3H, Me), 0.79 (s, 3H, Me). ^{19}F NMR ($CDCl_3$): δ −63.4 (d, J = 21.5 Hz). ^{13}C NMR (125 MHz, $CDCl_3$): δ 163.9 (Ar), 157.8 (Ar), 156.7 (Ar), 153.8 (Ar), 136.9 (Ar), 134.7 (d, J = 10.0 Hz, Ar), 133.5 (Ar), 133.3 (d, J = 42.8 Hz, Ar), 127.8 (d, J = 9.6 Hz, Ar), 126.8 (Ar), 124.7 (Ar), 122.2 (Ar), 118.1 (Ar), 118.0 (Ar), 52.1 (d, J = 21.5 Hz, PCH_2Ar), 46.5 (d, J = 42.8 Hz, PCH_2), 43.0 (CMe_2), 38.0 (CMe_3), 35.5 (CMe_2), 35.0 (CMe_3), 34.1 (t-Bu), 31.1 (t-Bu), 28.7 (d, J = 10.6 Hz, CMe_2).

DFT Calculations. Full details on the computational methods are provided in the Supporting Information.

X-ray Crystallography. Details for the seven crystal structures are given in the Supporting Information. All data were collected at 100 K (except for **2e**, which were collected at 200 K due to an apparent destructive phase change at lower temperatures) on Bruker diffractometers using Mo Kα radiation. For **4e**, **3b**, and **4b**, the program SQUEEZE was used to render highly disordered solvent molecules. All specimens of **2d** and **5a** were found to be rotationally twinned. The structure of **2e** contained a disordered t-Bu group.

■ ASSOCIATED CONTENT

Supporting Information

The Supporting Information is available free of charge on the ACS Publications website at DOI: 10.1021/acs.organomet.9b00425.

Complete experimental details supplemented with NMR spectra and specifics on DFT computational methodology (PDF)

Optimized Cartesian coordinates (XYZ)

Accession Codes

CCDC 1936294−1936299 and 1937111 contain the supplementary crystallographic data for this paper. These data can be obtained free of charge via www.ccdc.cam.ac.uk/data_request/cif, or by emailing data_request@ccdc.cam.ac.uk, or by contacting The Cambridge Crystallographic Data Centre, 12 Union Road, Cambridge CB2 1EZ, UK; fax: +44 1223 336033.

■ AUTHOR INFORMATION

Corresponding Author

*E-mail for M.F.C.: mfcain@hawaii.edu.

ORCID

Matthew F. Cain: 0000-0002-0673-5839

Author Contributions

‖J.I.P.L and L.S.W. contributed equally.

Notes

The authors declare no competing financial interest.

■ ACKNOWLEDGMENTS

M.F.C. thanks the University of Hawai'i at Mānoa (UHM) for generous start-up funds and laboratory space. M.F.C. also thanks the National Science Foundation (NSF) for a CAREER Award (NSF CHE-1847711). M.L.N. thanks the National Institute of Health for a fellowship funded by Grant U54CA143727. Mass spectroscopic data was obtained at UHM on an Agilent 6545 Accurate-Mass QTOF-LCMS (NSF CHE-1532310). R.P.H. thanks Dartmouth College for access to computational resources. Elemental analyses were conducted by William Brennessel (University of Rochester).

■ REFERENCES

(1) Ozawa, F.; Nakajima, Y. PNP-Pincer-Type Phosphaalkene Complexes of Late Transition Metals. *Chem. Rec.* **2016**, *16*, 2314−2323.

(2) Nakajima, Y.; Nakao, Y.; Sakaki, S.; Tamada, Y.; Ono, T.; Ozawa, F. Electronic Structure of Four-Coordinate Iron(I) Complex Supported by a Bis(phosphaethenyl)pyridine Ligand. *J. Am. Chem. Soc.* **2010**, *132*, 9934−9936.

(3) (a) Nakajima, Y.; Shiraishi, Y.; Tsuchimoto, T.; Ozawa, F. Synthesis and Coordination Behavior of Cu(I) Bis(phosphaethenyl)-pyridine Complexes. *Chem. Commun.* **2011**, *47*, 6332−6334.

DOI: 10.1021/acs.organomet.9b00425
Organometallics 2019, 38, 3338−3348

(b) Nakajima, Y.; Tsuchimoto, T.; Chang, Y.-H.; Takeuchi, K.; Ozawa, F. Reactions of [Cu(X)(BPEP-Ph)] (X = PF_6, SbF_6) with Silyl Compounds. Cooperative Bond Activation involving Non-Coordinating Anions. *Dalton Trans.* **2016**, *45*, 2079−2084.
(4) (a) Le Floch, P. Phosphaalkene, Phospholyl and Phosphinine Ligands: New Tools in Coordination Chemistry and Catalysis. *Coord. Chem. Rev.* **2006**, *250*, 627−681. (b) Lin, Y.-F.; Nakajima, Y.; Ozawa, F. Reduction of an Fe(I) Mesityl Complex Induced by π-Acid Ligands. *Dalton Trans.* **2014**, *43*, 9032−9037.
(5) Jouaiti, A.; Geoffroy, M.; Terron, G.; Bernardinelli, G. The Benzodiphosphaalkene Ligand and Its Pd(II) and Pt(II) Complexes: Their Synthesis, Structure, and an ESR Study of Their Reduction Potentials. *J. Am. Chem. Soc.* **1995**, *117*, 2251−2258.
(6) (a) Jouaiti, A.; Geoffroy, M.; Bernardinelli. 1,2-Bis[2-(2,4,6-tri-*tert*-butylphenyl)phosphanediylmethyl]benzene, L: Synthesis and Structure of L, of the chelated complex [$PdLCl_2$] and of a Derived Cyclometallated Chiral Complex. *Chem. Commun.* **1996**, 437−438. (b) van der Sluis, M.; Beverwijk, V.; Termaten, A.; Bickelhaupt, F.; Kooijman, H.; Spek, A. L. Synthesis of Novel Phosphaalkene-Based Bidentate Ligands Mes*P═CH(3-R-Ar) (R = Pyridyl, Carbaldimino) and Formation of Three-Membered Palladacycles Mes*(Me)P−CH(3-R-Ar)−PdCl by Carbapalladation of the P═C Double Bond. *Organometallics* **1999**, *18*, 1402−1407.
(7) Houdard, R.; Mézailles, N.; Le Goff, X.-F.; Le Floch, P. Platinum(0)-Catalyzed Intramolecular Addition of a C−H Bond onto the P═C Bond of a Phosphaalkene. *Organometallics* **2009**, *28*, 5952−5959.
(8) Notable exception: Bates, J. I.; Gates, D. P. Diphosphiranium (P_2C) or Diphosphetanium (P_2C_2) Cyclic Cations: Different Fates for the Electrophile-Initiated Cyclodimerization of a Phosphaalkene. *J. Am. Chem. Soc.* **2006**, *128*, 15998−15999.
(9) Jouaiti, A.; Geoffroy, M.; Terron, G.; Bernardinelli, G. Synthesis, Structure and Ligand-Centred Reduction of an Orthometallated Complex of Palladium containing Two Phosphaalkene Groups. *J. Chem. Soc., Chem. Commun.* **1992**, 155−156.
(10) Jouaiti, A.; Geoffroy, M.; Bernardinelli, G. Synthesis of New Chelating Agents: Association of a Phosphaalkene Moiety with a Pyridine. *Tetrahedron Lett.* **1992**, *33*, 5071−5074.
(11) Taguchi, H.; Chang, Y.-H.; Takeuchi, K.; Ozawa, F. Catalytic Synthesis of an Unsymmetrical PNP-Pincer-Type Phosphaalkene Ligand. *Organometallics* **2015**, *34*, 1589−1596.
(12) Chang, Y.-H.; Nakajima, Y.; Tanaka, H.; Yoshizawa, K.; Ozawa, F. Facile N−H Bond Cleavage of Ammonia by an Iridium Complex Bearing a Noninnocent PNP-Pincer Type Phosphaalkene Ligand. *J. Am. Chem. Soc.* **2013**, *135*, 11791−11794.
(13) Gunanathan, C.; Milstein, D. Metal−Ligand Cooperation by Aromatization−Dearomatization: A New Paradigm in Bond Activation and "Green" Catalysis. *Acc. Chem. Res.* **2011**, *44*, 588−602.
(14) Chang, Y.-H.; Nakajima, Y.; Tanaka, H.; Yoshizawa, K.; Ozawa, F. Mechanism of N−H Bond Cleavage of Aniline by a Dearomatized PNP-Pincer Type Phosphaalkene Complex of Iridium(I). *Organometallics* **2014**, *33*, 715−721.
(15) Nakajima, Y.; Okamoto, Y.; Chang, Y.-H.; Ozawa, F. Synthesis, Structures, and Reactivity of Ruthenium Complexes with PNP-Pincer Type Phosphaalkene Ligands. *Organometallics* **2013**, *32*, 2918−2925.
(16) Gunanathan, C.; Milstein, D. Bond Activation and Catalysis by Ruthenium Pincer Complexes. *Chem. Rev.* **2014**, *114*, 12024−12087.
(17) (a) Synthesis of **1b**: Yam, M.; Chong, J. H.; Tsang, C.-W.; Patrick, B. O.; Lam, A. E.; Gates, D. P. Scope and Limitations of the Base-Catalyzed Phospha-Peterson P═C Bond Formation Reaction. *Inorg. Chem.* **2006**, *45*, 5225−5234. (b) . Synthesis of **1c**: ref 22.
(18) Dugal-Tessier, J.; Dake, G. R.; Gates, D. P. P,N-Chelate Complexes of Pd(II) and Pt(II) Based on a Phosphaalkene Motif: A Catalyst for the Overman−Claisen Rearrangement. *Organometallics* **2007**, *26*, 6481−6486.
(19) Takeuchi, K.; Minami, A.; Nakajima, Y.; Ozawa, F. Synthesis and Structures of Nickel Complexes with a PN-Chelate Phosphaalkene Ligand. *Organometallics* **2014**, *33*, 5365−5370.
(20) (a) Shah, S.; Protasiewicz, J. D. 'Phospha-Wittig' Reactions using Isolable Phosphoranylidenephosphines ArP═PR_3 (Ar = 2,6-$Mes_2C_6H_3$ or 2,4,6-$Bu^t_3C_6H_2$). *Chem. Commun.* **1998**, 1585−1586. (b) Shah, S.; Protasiewicz, J. D. 'Phospha-Variations' on the Themes of Staudinger and Wittig: Phosphorus Analogs of Wittig Reagents. *Coord. Chem. Rev.* **2000**, *210*, 181−201.
(21) All 6-substituted pyridine-2-carboxyaldehyde derivatives are commercially available.
(22) Ligand **2a** had previously been synthesized by a phospha-Peterson methodology: van der Sluis, M.; Beverwijk, V.; Termaten, A.; Gavrilova, E.; Bickelhaupt, F.; Kooijman, H.; Veldman, N.; Spek, A. L. Synthesis of 2-(2-Pyridyl)phosphaalkenes [Mes*P═C(R)Py] (R = H, $SiMe_3$) and Their Complexes η^1,η^1-[Mes*P═C(R)Py]-XPdCl (X = Cl, Me, Ac). *Organometallics* **1997**, *16*, 1144−1152.
(23) Comparable bond lengths found: (a) Magnuson, K. W.; Oshiro, S. M.; Gurr, J. R.; Yoshida, W. Y.; Gembicky, M.; Rheingold, A. L.; Hughes, R. P.; Cain, M. F. Streamlined Preparation and Coordination Chemistry of Hybrid Phosphine-Phosphaalkene Ligands. *Organometallics* **2016**, *35*, 855−859. (b) Deschamps, E.; Deschamps, B.; Dormieux, J. L.; Ricard, L.; Mézailles, N.; Le Floch, P. 4,6-Bis(supermesitylphosphanylidenemethyl)dibenzofuran. Synthesis, X-ray Structure and Reactivity towards Group 11 Metals. *Dalton Trans.* **2006**, 594−602.
(24) Shorter bond lengths found: (a) Miura-Akagi, P. M.; Nakashige, M. L.; Maile, C. K.; Oshiro, S. M.; Gurr, J. R.; Yoshida, W. Y.; Royappa, A. T.; Krause, C. E.; Rheingold, A. L.; Hughes, R. P.; Cain, M. F. Synthesis of a Tris(phosphaalkene)phosphine Ligand and Fundamental Organometallic Rewactions on Its Sterically Shielded Metal Complexes. *Organometallics* **2016**, *35*, 2224−2231. (b) Dugal-Tessier, J.; Dake, G. R.; Gates, D. P. Chiral Ligand Design: A Bidentate Ligand Incorporating an Acyclic Phosphaalkene. *Angew. Chem., Int. Ed.* **2008**, *47*, 8064−8067. (c) Gudimetla, V. B.; Rheingold, A. L.; Payton, J. L.; Peng, H.-L.; Simpson, M. C.; Protasiewicz, J. D. Photochemical *E-Z* Isomerization of *meta*-Terphenyl-Protected Phosphaalkenes and Structural Characterizations. *Inorg. Chem.* **2006**, *45*, 4895−4901.
(25) (a) Reference 15. (b) Campian, M. V.; Perutz, R. N.; Procacci, B.; Thatcher, R. J.; Torres, O.; Whitwhood, A. C. Selective Photochemistry at Stereogenic Metal and Ligand Centers of *cis*-[Ru(diphosphine)$_2$(H)$_2$]: Preparative, NMR, Solid State, and Laser Flash Studies. *J. Am. Chem. Soc.* **2012**, *134*, 3480−3497.
(26) van der Boom, M. E.; Iron, M. A.; Atasoylu, O.; Shimon, L. J. W.; Rozenberg, H.; Ben-David, Y.; Konstantinovski, L.; Martin, J. M. L.; Milstein, D. sp^3 C−H and sp^2 C−H Agostic Ruthenium Complexes: A Combined Experimental and Theoretical Study. *Inorg. Chim. Acta* **2004**, *357*, 1854−1864.
(27) Major, Q.; Lough, A. J.; Gusev, D. G. Substituent Effects in POP Pincer Complexes of Ruthenium. *Organometallics* **2005**, *24*, 2492−2501.
(28) Perera, S. D.; Shaw, B. L. A General Method of Promoting Agostic Interactions (Ru←H_a−C) using Azine Phosphines. *J. Chem. Soc., Chem. Commun.* **1994**, *0*, 1201−1202.
(29) Huang, D.; Streib, W. E.; Bollinger, J. C.; Caulton, K. G.; Winter, R. E.; Scheiring, T. 14-Electron Four-Coordinate Ru(II) Carbyl Complexes and Their Five-Coordinate Precursors: Synthesis, Double Agostic Interactions, and Reactivity. *J. Am. Chem. Soc.* **1999**, *121*, 8087−8097.
(30) Baratta, W.; Herdtweck, E.; Rigo, P. [$RuCL_2${PPh_2(2,6-$Me_2C_6H_3$)}$_2$]: A Neutral 14-Electron Ruthenium(II) Complex with Two Agostic Interactions. *Angew. Chem., Int. Ed.* **1999**, *38*, 1629−1631.
(31) Herrera, A.; Grasruck, A.; Heinemann, F. W.; Scheurer, A.; Chelouan, A.; Frieβ, S.; Seidel, F.; Dorta, R. Developing P-Stereogenic, Planar−Chiral P-Alkene Ligands: Monodentate, Bidentate, and Double Agostic Coordination Modes on Ru(II). *Organometallics* **2017**, *36*, 714−720.
(32) Brookhart, M.; Green, M. L. H.; Parkin, G. Agostic Interactions in Transition Metal Compounds. *Proc. Natl. Acad. Sci. U. S. A.* **2007**, *104*, 6908−6914.

DOI: 10.1021/acs.organomet.9b00425
Organometallics 2019, 38, 3338−3348

(33) For a related Pt−CF_3 interaction, see: Phillips, I. G.; Ball, R. G.; Cavell, R. G. Preparation and Characterization of Triphospholene Complexes of Zerovalent Platinum: Crystal and Molecular Structure of $[Pt\{(CF_3)P(CF_3)P(CF_3)PC(CF_3)=C(CF_3)\}(PPh_3)_2]$. *Inorg. Chem.* **1987**, *26*, 4074−4079.
(34) Perera, S. D.; Shaw, B. L. A Systematic Method of Promoting an Aryl Fluoride to Coordinate to Ruthenium(II). *Inorg. Chim. Acta* **1995**, *228*, 127−131.
(35) Plenio, H. The Coordination Chemistry of the CF Unit in Fluorocarbons. *Chem. Rev.* **1997**, *97*, 3363−3384.
(36) Stanek, K.; Czarniecki, B.; Aardoom, R.; Rüegger, H.; Togni, A. Remote C−F−Metal Interactions in Late-Transition-Metal Complexes. *Organometallics* **2010**, *29*, 2540−2546.
(37) Birkholz, M.-N.; Freixa, Z.; van Leeuwen, P. W. N. M. Bite Angle Effects of Diphosphines in C−C and C−X Bond Formation Cross Coupling Reactions. *Chem. Soc. Rev.* **2009**, *38*, 1099−1118.
(38) Addison, A. W.; Rao, T. N.; Reedijk, J.; van Rijn, J.; Verschoor, G. C. Synthesis, Structure, and Spectroscopic Properties of Copper(II) Compounds Containing Nitrogen-Sulphur Donor Ligands: the Crystal and Molecular Structure of Aqua[1,7-bis(*N*-methylbenzimidazol-2′-yl)-2,6-dithiaheptane]copper(II) Perchlorate. *J. Chem. Soc., Dalton Trans.* **1984**, 1349−1356.
(39) This behavior is typical of phosphaalkenes. See refs 23a and 24a.
(40) Bent, H. A. An Appraisal of Valence-Bond Structures and Hybridization in Compounds of the First-Row Elements. *Chem. Rev.* **1961**, *61*, 275−311.
(41) Deegan, M. M.; Muldoon, J. A.; Hughes, R. P.; Glueck, D. S.; Rheingold, A. L. Synthesis and Structure of Metal Complexes of P-Stereogenic Chiral Phosphiranes: An EDA-NOCV Analysis of the Donor-Acceptor Properties of Phosphirane Ligands. *Organometallics* **2018**, *37*, 1473−1482.
(42) Ficks, A.; Clegg, W.; Harrington, R. W.; Higham, L. J. Air-Stable Chiral Primary Phosphines: A Gateway to MOP Ligands with Previously Inaccessible Stereoelectronic Profiles. *Organometallics* **2014**, *33*, 6319−6329.
(43) Coe, B. J.; Glenwright, S. J. Trans-Effects in Octahedral Transition Metal Complexes. *Coord. Chem. Rev.* **2000**, *203*, 5−80.
(44) See, R. F.; Kozina, D. Quantification of the Trans Influence in d^8 Square Planar and d^6 Octahedral Complexes: A Database Study. *J. Coord. Chem.* **2013**, *66*, 490−500.
(45) Some related complexes with a highly pyramidalized five-membered P-containing ring: (a) Panichakul, D.; Mathey, F. Serendipitous Discovery of a Phosphirene-Phosphindole Rearrangement. *Organometallics* **2011**, *30*, 348−351. (b) Nguyen, D. H.; Lauréano, H.; Jugé, S.; Kalck, P.; Daran, J.-C.; Coppel, Y.; Urrutigoity, M.; Gouygou, M. First Dibenzophospholyl(diphenylphosphino)-methane−Borane Hybrid P−(η^2-BH_3) Ligand: Synthesis and Rhodium(I) Complex. *Organometallics* **2009**, *28*, 6288−6292.
(46) (a) Mann, F. G.; Millar, I. T. The Synthesis of 1-Substituted Phosphindolines. *J. Chem. Soc.* **1951**, 2205−2206. (b) Symmes, C.; Quin, L. D. 1-Vinylcycloalkenes in the McCormack Cycloaddition with Phosphonous Dihalides. Stereochemistry of Some Resulting Bicyclic Phospholene Oxides. *J. Org. Chem.* **1976**, *41*, 238−242.
(47) With a meta-substituted bisphosphinoarene ligand: Dani, P.; Toorneman, M. A. M.; van Klink, G. P. M.; van Koten, G. Complexes of Bis-*ortho*-cyclometalated Bisphosphinoaryl Ruthenium(II) Cations with Neutral *Meta*-bisphosphinoarene Ligands Containing an Agostic C−H•••Ru Interaction. *Organometallics* **2000**, *19*, 5287−5296.
(48) Crossley, I. R.; Hill, A. F.; Humphrey, E. R.; Smith, M. K. A Less Carbocentric View of Agostic Interactions: The Complexes $[Rh(\eta^4\text{-cod})\{H_2A(mt)_2\}]$ (A = B, C^+; mt = Methimazolyl). *Organometallics* **2006**, *25*, 2242−2247.
(49) (a) Brookhart, M.; Green, M. L. H. Carbon-Hydorgen-Transition Metal Bonds. *J. Organomet. Chem.* **1983**, *250*, 395−408. (b) Häller, L. J. L.; Page, M. J.; Macgregor, S. A.; Mahon, M. F.; Whittlesey, M. K. Activation of an Alkyl C−H Bond Geminal to an Agostic Interaction: An Unusual Mode of Base-Induced C−H Avtivation. *J. Am. Chem. Soc.* **2009**, *131*, 4604−4605.
(50) Tsang, C.-W.; Rohrick, C. A.; Saini, T. S.; Patrick, B. O.; Gates, D. P. Reactions of Electrophiles with the Phosphaalkene Mes*P=CH_2: Mechanistic Studies of a Catalytic Intramolecular C−H Bond Activation Reaction. *Organometallics* **2002**, *21*, 1008−1010.
(51) The related electrophilic activation of phosphaalkenes implicating phosphenium-type intermediates was reported here: Tsang, C.-W.; Rohrick, C. A.; Saini, T. S.; Patrick, B. O.; Gates, D. P. Destiny of Transient Phosphenium Ions Generated from the Addition of Electrophiles to Phosphaalkenes: Intramolecular C−H Activation, Donor−Acceptor Formation, and Linear Oligomerization. *Organometallics* **2004**, *23*, 5913−5923.
(52) An example of a seven-coordinate, Ru(IV) complex: Duan, L.; Fischer, A.; Xu, Y.; Sun, L. Isolated Seven-Coordinate Ru(IV) Dimer Complex with $[HOHOH]^-$ Bridging Ligand as an Intermediate for Catalytic Water Oxidation. *J. Am. Chem. Soc.* **2009**, *131*, 10397−10399.
(53) Ben-Ari, E.; Leitus, G.; Shimon, L. J. W.; Milstein, D. Metal−Ligand Cooperation in C−H and H_2 Activation by an Electron-Rich PNP Ir(I) System: Facile Ligand Dearomatization−Aromatization as Key Steps. *J. Am. Chem. Soc.* **2006**, *128*, 15390−15391.
(54) Khaskin, E.; Iron, M. A.; Shimon, L. J. W.; Zhang, J.; Milstein, D. N−H Activation of Amines and Ammonia by Ru via Metal−Ligand Cooperation. *J. Am. Chem. Soc.* **2010**, *132*, 8542−8543.
(55) Balaraman, E.; Gnanaprakasam, B.; Shimon, L. J. W.; Milstein, D. Direct Hydrogenation of Amides to Alcohols and Amines under Mild Conditions. *J. Am. Chem. Soc.* **2010**, *132*, 16756−16758.
(56) Cowley, A. H.; Norman, N. C.; Pakulski, M. Phosphorus Compounds Containing Sterically Demanding Groups. *Inorg. Synth.* **2007**, *27*, 235−240.

DOI: 10.1021/acs.organomet.9b00425
Organometallics 2019, 38, 3338−3348